APPLICATION TO ROTARY WINGS OF A SIMPLIFIED AERODYNAMIC LIFTING SURFACE THEORY FOR UNSTEADY COMPRESSIBLE FLOW

B. M. Rao* and W. P. Jones**
Department of Aerospace Engineering
Texas A&M University, College Station, Texas

Abstract

In a recent paper, Jones and Moore have developed a simple numerical lifting surface technique for calculating the aerodynamic coefficients on oscillating wings in subsonic flight. The method is based on the use of the full lifting surface theory and is not restricted in any way as to frequency, mode of oscillation or aspect ratio when $M < 1$. In this study, this simple but general method of predicting airloads is applied to helicopter rotor blades on a full three-dimensional basis. The general theory is developed for a rotor blade at the $\psi = \pi/2$ position where flutter is most likely to occur. Calculations of aerodynamic coefficients for use in flutter analysis are made for forward and hovering flight with low inflow for Mach numbers 0 and 0.8 and frequency ratios p/Ω=1 and 4. The results are compared with values given by two-dimensional strip theory for a rigid rotor hinged at its root. The comparisons indicate the inadequacies of strip theory for airload prediction. One important conclusion drawn from this study is that the curved wake has a substantial effect on the chordwise load distribution. The pitching moment aerodynamic coefficients differ appreciably from the results given by strip theory.

Introduction

In a survey paper, Ref. 1, Jones' et al. give a detailed account of significant developments in the field of unsteady aerodynamics of helicopter rotor blades. One of the problem areas surveyed was that of blade flutter as it has been found that under certain operating conditions, rotor blades can flutter in both hovering and forward flight. This phenomenon has been investigated by several researchers in Refs. 2, 3, 4, and 5 and the results of their studies have improved our understanding of the problem. For the case of hovering flight, J. P. Jones in Ref. 2 applied a method developed by W. P. Jones in Ref. 6 to derive the approximate aerodynamic coefficients for an oscillating single rotor blade for use in his flutter analysis. He approximated the actual flow conditions by neglecting curvature effects and assuming a simple two-dimensional mathematical model cosisting of a reference blade and an infinite number of wakes lying beneath the reference blade extending from $-\infty$ to ∞. He considered flapping and pitching motions and compared his results with those obtained experimentally by Daughaday and Kline in Ref. 3. On the basis of this work it was concluded that the wake is primarily responsible for some of the vibratory phenomena found on helicopters in practice. For low inflow conditions, Loewy in Ref. 4 used a similar mathematical model to that of J. P. Jones and investigated the variation in the pitching moment damping coefficient of a particular blade section as p/Ω varied for specified positions of axis of oscillation and a range of values of wake spacing. He found that the damping coefficient became negative whenever p/Ω was slightly greater than an integer for axis of oscillation forward of quarter-chord. Similarly he found that the damping coefficient for a flapping oscillation dropped sharply at integral values of p/Ω but did not actually become negative. Timman and Van de Vooren in Ref. 5, on the other hand, assumed that there was no inflow through the rotor disk and developed a theory for calculating the aerodynamic forces on a blade rotating through its own wake. Their results agree with those obtained in Refs. 2 and 4 in the limit when zero spacing between the wakes is assumed. All this theoretical work confirms the conclusion that the proximity of the wake is a contributing factor to rotor blade flutter.

All the theoretical work described above is based on the assumption that the flow is incompressible. However, with the advent of helicopters capable of flying with blade tip speeds ranging up to and in excess of the speed of sound, compressibility effects need to be taken into account when determining coefficients for use in flutter analysis. Jones and Rao in Ref. 7 were able to do this on the basis of two-dimensional theory and have derived coefficients for a range of Mach numbers, reduced frequencies, and wake spacing. Their analysis is based on the use of Loewy's model, Ref. 4, of the helical wake and the application of a theory developed earlier by Jones in Ref.8 for an oscillating airfoil in compressible flow. The values of the coefficients given in Ref. 7 agree with those obtained in Refs. 2 and 4 for zero Mach number but differ appreciably when the Mach number is varied. Hammond in Ref. 9 also developed a theory for determining compressibilty effects by using a different model of flow from that used in Ref. 7. In his model, the wake of the qth blade of a Q bladed rotor after n revolutions extends from $-2\pi(n+q/Q)$ to ∞; in Jones and Rao's model it extends from $-\infty$ to ∞. His aerodynamic coefficients for several Mach numbers and inflow ratios are in general agreement with the results of Jones and Rao in Ref. 7.

While the aerodynamic derivatives predicted by two-dimensional strip theory are widely used in predicting the flutter speeds of helicopter rotor blades, the method does not allow for curvature and finite aspect ratio effects. For incompressible flow, Ashley, Moser, and Dugundji in Ref. 10 developed a three-dimensional model in which they

Presented at the AHS/NASA-Ames Specialists' Meeting on Rotorcraft Dynamics, February 13-15, 1974. The funds for computation were provided by the U. S. Army Research Office, Durham.

* Associate Professor
** Distinguished Professor

modified Reissner's theory, Ref. 11, for oscillating wings in rectilinear flow by including the free stream velocity variations along the span. Their results indicate a negligible difference between two and three-dimensional solutions up to 95% of the span. Jones and Rao in Ref. 12 similarly studied tip vortex effects in compressible flow and they also concluded that such effects are negligible except in regions close to the tip. In some of his earlier work, Miller in Refs. 13, 14, and 15, developed a helical wake model in which the rotor wake was divided into a "near" wake and a "far" wake. The near wake included the portion attached to the blade that extend approximately one-quarter of a revolution from the blade trailing edge. The effects of the near wake include an induced chordwise variation in downwash and were formulated using an adoptation of Loewy's strip theory. The chordwise variation in the velocity over the airfoil induced by the far wake was neglected. Miller extended his model to study the forward flight case and found that the nonuniform downwash induced at the rotor disk by the wake vortex system could account for the higher harmonic airloads encountered on rotor blades in forward flight. He also showed that under certain conditions of low inflow and low speed transition flight the returning wake could be sucked up into the leading edge of the rotor which would account for some of the vibration and noise. Piziali in Ref. 16 has developed an alternative numerical method in which the wake of a rotor blade is represented by discrete straight line shed and trailing vortex elements. He satisfied the chordwise boundary conditions, but the rotor blade was limited to one degree of freedom in flapping. Sadler in Ref. 17, using a model similar to Piziali's, developed a method for predicting the helicopter wake geometry at a "start up" configuration. He represented the wake by a fine mesh of transverse and trailing vortices starting with the first movement of the rotor blade generating a bound vortex, and, to preserve zero total vorticity, a corresponding shed vortex in the wake. Integrating the mutual interference of the trailing and shed vortices upon each other over small intervals of time, Sadler was able to predict a wake geometry. Although his model showed fair agreement with the available experimental data for advance ratios above one-tenth, Sadler's method is limited due to the large computational time required to represent the wake by a finite mesh.

Though many forms of flutter can occur on rotor blades, attention in this report is concentrated on the determination of appropriate aerodynamic coefficients for use in the analysis of blade flutter of the classical bending-torsion type. Shipman and Wood in Ref. 20 have considered this problem but they did not take compressibilty and finite span effects into account. The two-dimensional mathematical model used is similar to that employed by other authors except that they assumed that flutter would first occur when the relative velocity over the rotor blade reaches its critical value when $\psi \simeq \pi/2$. For greater or lower values of ψ, the relative speed would be reduced below the critical speed for flutter and any incipient growing flutter oscillation would be damped. This reasoning led them to represent the blade motion by a series of oscillatory pulses, where each disturbance occurs over the range, $\frac{\pi}{2} - \Delta\psi_1 < \psi < \frac{\pi}{2} + \Delta\psi_2$. Corresponding to each burst of oscillation, packets of vorticity are assumed to be shed into the wake. With increasing forward speed, the spacing between the packets of vorticity also increases and it was found that the flutter speed became constant when μ, the advance ratio, was above 0.2. The approach used in the present study differs from that adopted by Shipman and Wood in that continuous high frequency small oscillations are assumed to be superimposed on the normal periodic motion of the blade. The airloads and aerodynamic derivatives associated with the perturbed oscillation of the rotor blade can then be calculated by the method described in this paper. Since the rotor blade will first attain its critical speed for classical flutter at $\psi \simeq \pi/2$, the aerodynamic derivatives corresponding to this value of ψ only have been calculated. The method takes finite aspect ratio and subsonic compressibility effects fully into account. Typical results for a rotor blade hinged at its root describing flapping and twisting oscillations are given for a range of Mach numbers and frequency values.

Basic Equations

In the development of the analysis of the Jones-Moore theory, Ref. 18, for oscillating wings in rectilinear flight, the space variables x, y, z, and t are replaced by X, Y, Z, and T, respectively, so that

$$x = \ell X, \quad y = \frac{\ell Y}{\beta}, \quad z = \frac{\ell Z}{\beta}, \quad t = \frac{\ell T}{U} \tag{1}$$

where ℓ is a convenient reference length, U is the uniform velocity, M is the Mach number and $\beta = (1-M^2)^{1/2}$. The velocity potential of the flow around a surface oscillating at a frequency p can then be expressed as

$$\phi(x,y,z,t) = U\ell\Phi(X,Y,Z)e^{i(\lambda X + \omega T)} \tag{2}$$

where $\omega = p\ell/U$, $\lambda = M^2\omega/\beta^2$. The function Φ may be regarded as a modified velocity potential. Furthermore, it can be shown that it satisfies the wave equation

$$\frac{\partial^2\Phi}{\partial X^2} + \frac{\partial^2\Phi}{\partial Y^2} + \frac{\partial^2\Phi}{\partial Z^2} + \kappa^2\Phi = 0 \tag{3}$$

where $\kappa = M\omega/\beta^2$.

Since in this problem the motion of the surface is assumed to be prescribed, the downwash velocity at any point on it must be the same as the downwash induced by the velocity (or doublet) distribution over the surface and its wake. This condition must be satisfied in order to ensure tangential flow over the surface at all points. It is also assumed that the rotor blade is a thin surface oscillating about its equilibrium position in the plane z = 0. If $\zeta = \zeta' e^{ipt}$ defines the downwash displacement at any point (x,y) at time t, this boundary condition requires that the downward velocity and $\partial\phi/\partial z$ must be equal. In the transformed coordinates, this implies that

$$W = \frac{\partial \Phi}{\partial Z} = \frac{we^{-i(\lambda X + \omega T)}}{U\beta} \qquad (4)$$

where $w = \frac{\partial \zeta}{\partial t} + U\frac{\partial \zeta}{\partial x}$ is known.

A further condition that must be imposed on any solution is that it leads to zero pressure difference across the wake created by the oscillating surface. From the general equations of flow it can be established that the local lift $\tilde{\ell}(x,y,t)$ at any point is given by

$$\tilde{\ell}(x,y,t) = \rho\left(\frac{\partial k}{\partial t} + U\frac{\partial k}{\partial x}\right) \qquad (5)$$

where $k = \phi_u - \phi_\ell$, the discontinuity in the velocity potential. From Eq. (5), it immediately follows that on the surface

$$\tilde{\ell}(x,y,t) = \rho U^2\left(i\nu K + \frac{\partial K}{\partial X}\right) e^{i(\lambda X + \omega T)} \qquad (6)$$

where $\nu = \omega/\beta^2$ and $K = \Phi_u - \Phi_\ell$. This yields

$$i\nu K + \frac{\partial K}{\partial X} = 0 \qquad (7)$$

everywhere in the wake since the lift must then be zero. From Eq. (7), it can be deduced that at any point in the wake

$$K(X,Y) = K(X_t,Y)\, e^{-i\nu(X-X_t)} \qquad (8)$$

where $X = X_t$ denotes the position of the trailing edge of the section at Y.

As shown in Ref. 19, the solution of Eq. (3) may then be derived from the integral equation

$$4\pi W(X_p,Y_p,0) = \iint_{Z\to 0} K(X,Y)\frac{\partial^2}{\partial Z^2}\left(\frac{e^{-i\kappa\xi}}{\xi}\right)dXdY \qquad (9)$$

where W is the modified downwash at the point X_p,Y_p given by Eq. (4), K has to take the form specified by Eq. (8) at points in the wake and $\xi = [(X-X_p)^2 + (Y-Y_p)^2 + Z^2]^{1/2}$.

The double integral in Eq. (9) must be taken over the area of the oscillating surface and its wake. It should be remembered, however, that K = 0 along the leading edge and the sides of the area of integration.

In the numerical technique developed in Ref. 18 for calculating the airloads on oscillating wings in rectilinear flight, the wing is divided into a number of conveniently shaped boxes and K is assumed to be constant over each box. The wake, on the other hand, is divided into a number of chordwise strips and K over each strip is defined by Eq. (8). The contribution of the wake to the downwash $W(X_p,Y_p)$ is then derived by direct numerical integration.

The application of the method outlined above to determine the airloads on rotor blades presents certain difficulties, the principal one being that the flow velocity over the rotor blades is not constant as assumed in the derivation of Eqs. (3) and (8) for wings in straight flight. To overcome this difficulty, it is assumed that the rotor blade can be represented by a number of spanwise segments over every one of which the flow is taken to have its average value and appropriate Mach number. On this basis the above analysis can be modified for application to rotor blades as outlined in the next section.

Rotor Blade Theory

In the present analysis, the rotor blade is taken to be fixed at the $\psi = \pi/2$ position and its helical wake is assumed to extend rearwards as indicated in Fig. 1. Normally, one would expect the vorticity shed by the perturbed blade to be carried downstream by the distorted wake of the loaded rotor blade. However, in the present preliminary study, uniform inflow is assumed and any distortion of the wake due to blade-tip vortex interference is ignored. The aerodynamic coefficients corresponding to any prescribed motion can then be calculated for forward and hovering flight by the method described below.

a) Forward Flight (Rotor Blade at $\psi = \pi/2$)

Let R denote the tip radius of the blade and assume $x = Rx'$, $y = Ry'$, and $z = Rz'$. For forward flight with velocity V, the relative local velocity at section y will be denoted by $U(=V+\Omega Ry')$ and $U'(=\mu+y')$, where Ω is the angular rotation and $\mu(=V/\Omega R)$ is the advance ratio. It then follows that at the section y'_p, the downwash $w(x'_p,y'_p)$ is given by

$$w(x'_p,y'_p) = \Omega R\left(i\frac{p}{\Omega}\zeta' + U'\frac{\partial \zeta'}{p\partial x'}\right) e^{ipt} \qquad (10)$$

where $\zeta = R\zeta' e^{ipt}$ is the displacement of the blade at the point, (x'_p,y'_p). When the blade is describing flapping and twisting motions, ζ' may be expressed as

$$\zeta' = \gamma' f(y') + x'\alpha' F(y') \qquad (11)$$

where γ' and α' are the amplitudes at the reference section and f(y') and F(y') are the modes of flapping and twisting oscillations, respectively. If the blade is assumed to be rigid and hinged at the root, f(y') = y', and F(y') = 1 in the above equation. For convenience, the reference section is taken to be at the tip but, in actual flutter calculations, the section at 0.8R would be a better choice.

To obtain the distribution of K corresponding to the motion prescribed by Eq. (10), Eq. (9) is first expressed in terms of the original variables and K is replaced by $Rk'e^{ipt}$. It may then be written as

$$\frac{4\pi w' e^{-i\lambda' x'_p}}{\beta_p} = \iint k'(x',y')e^{-i\lambda' x'}\frac{\partial^2}{\partial z'^2}\left(\frac{e^{-i\kappa' r'}}{r'}\right)\frac{dx'dy'}{\beta} \qquad (12)$$

where $\kappa' = \frac{Mp}{\beta^2\Omega U'}$, $\lambda' = M\kappa'$, $w = w'e^{ipt}$, $\beta^2 = 1-M^2$, and $r' = [(x'-x'_p)^2 + \beta^2(y'-y'_p)^2 + \beta^2 z'^2]^{1/2}$.

The above equation can be used to obtain the solution to the problem of determining the flow over a rotor blade with a rectilinear wake. Since

the wake can withstand no lift, the condition, $\frac{\partial k}{\partial t} + U\frac{\partial k}{\partial x} = 0$, must be satisfied. For a rectilinear wake, this yields

$$k'(x',y') = k'_t(y')e^{-i\frac{p(x'-x'_t)}{\Omega U'}} . \quad (13)$$

However, if the wake originating from a blade strip is assumed to be curved

$$k'(s',y') = k'_t(y')e^{-i\frac{p(s'-s'_t)}{\Omega q'}} , \quad (14)$$

where $q' = (\mu^2 + y'^2 + 2\mu y'\sin\psi)^{1/2}$, $s = Rs'$ is the distance along the vortex path and y' specifies the spanwise location of the blade strip.

For computational purposes, Eq. (12) may be conveniently expressed as

$$4\pi\bar{W}(x'_p,y'_p) = \int\int\bar{K}(x',y')\frac{G}{\beta}\,dx'dy', \quad (15)$$

where $\bar{W}(x'_p,y'_p) = \frac{w(x'_p,y'_p)}{\beta_p}e^{-i\lambda'x'_p}$,

$\bar{K}(x',y') = k'(x',y')\,e^{-i\lambda'x'}$, and

$$G = \frac{\partial^2}{\partial z'^2}\left(\frac{e^{-ik'r'}}{r'}\right) = -\beta^2\left(\frac{e^{-ik'r'}}{r'}\right)\left[\,(1+ik'r')\left(1-\frac{3\beta^2z'^2}{r'^2}\right) + \kappa'^2\beta^2z'^2\,\right].$$

It should be noted that in the wake

$$\bar{K}(x',y') = \bar{K}_t(y')\,e^{-i\frac{\nu'(s'-s'_t)}{q'}} , \quad (16)$$

where $\nu' = \frac{p}{\Omega\beta^2}$.

b) Hovering Flight

For the simplest case of hovering flight, $\mu = 0$ and $s' = y'\theta$. Hence Eqs. (10), (11), (12), (13), and (15) can be simply modified by replacing μ with zero. Eqs. (14) and (16) then become

$$k'(\theta,y') = k'_t(y')\,e^{-i\frac{p}{\Omega}(\theta-\theta_t)} \quad (17)$$

and $$\bar{K}(\theta,y') = \bar{K}'_t(y')\,e^{-i\nu'(\theta-\theta_t)} , \quad (18)$$

where y' defines the location of the blade strip from which the wake originates.

Method Of Solution

The schematic diagram of the oscillating rotor blade is shown in Fig. 1. Eqs. (15) and (16) are combined and expressed as

$$4\pi\bar{W}(x'_p,y'_p) = -\int\int_{\text{blade surface}}\bar{K}(x',y')\beta\left(\frac{e^{-ik'r'_s}}{r'^3_s}\right)(1+ik'r'_s)\,dx'dy' + \int\int_{\text{wake}}\bar{K}_t(y')e^{-i\frac{\nu'(s'-s'_t)}{q'}}\beta\left(\frac{e^{-ik'r'_w}}{r'^3_w}\right)$$

$$\left[\,(1+ik'r'_w)\left(1-\frac{3\beta^2z'^2}{r'^2_w}\right) + \kappa'^2\beta^2z'^2\,\right] ds'dn', \quad (19)$$

where $r'_s = [\,(x'-x'_p)^2 + \beta^2(y'-y'_p)^2\,]^{1/2}$

$r'_w = [\,(x'-x'_p)^2 + \beta^2(y'-y'_p)^2 + \beta^2z'^2\,]^{1/2}$

$ds' = (dx'^2+dy'^2)^{1/2}$

and dn' is perpendicular to ds' and approximately equal to dy' on blade. The rotor blade is divided into a number of rectangular boxes (M x N) on which the doublet strengths are assumed to be constant as in Ref. 18. Based on this assumption, Eq. (19) can be expressed as

$$4\pi\bar{W}_{mn} = \sum_{i=1}^{}\sum_{j=1}^{}S_{ij}\bar{K}_{ij} + \sum_{j=1}^{}T_j\bar{K}_{tj} \quad (20)$$

In Eq. (20) S_{ij} and T_j may be interpreted as the aerodynamic influence coefficients and the actual expressions are given later in this section. S_{ij} T_j are the downwash velocities induced at the box mn due to the unit strength doublets located at the box ij and the wake strip j respectively. $\bar{K}_{ij}$ and $\bar{K}_{tj}$ are the doublet strengths at the box ij and the trailing edge of the wake strip j, respectively. With the use of the wake boundary condition, $\bar{K}_{tj}$ can be expressed as

$$\bar{K}_{tj} = \bar{K}_{Mj}/[e^{-i\frac{\nu'(x'_{tj}-x'_{Mj})}{U'_j}} + 2i\frac{\nu'(x'_{tj}-x'_{Mj})}{U'_j}] \quad (21)$$

Eqs. (20) and (21), then yield

$$4\pi\bar{W}_{mn} = \sum_{i=1}^{}\sum_{j=1}^{}A_{ij}\bar{K}_{ij} \quad (22)$$

where $A_{ij} = S_{ij}$ for $i \neq M$

and $A_{ij} = S_{ij} + T_j/[e^{-i\frac{\nu'(x'_{tj}-x'_{Mj})}{U'_j}} + 2i\frac{\nu'(x'_{tj}-x'_{Mj})}{U'_j}]$

for $i = M$.

For a given mode shape ($\bar{W}_{mn}$'s are known), Eq. (22) represents a system of M x N linear algebraic equations, the solution of which yields the values for $\bar{K}_{mn}$'s. M and N denote the total number of chordwise and spanwise stations respectively.

Once the appropriate $\bar{K}$ distribution has been found, it is then relatively easy to determine the aerodynamic forces per unit span acting on the rotor blade. If, in Eq. (5), $k = Rk'e^{ipt} = R\bar{K}e^{ipt}e^{i\lambda'x'}$, it then follows that the local lift $L(y) = L'(y)\,e^{ipt}$ and the nose-up pitching moment, $M(y) = M'(y)\,e^{ipt}$, referred to the mid-point of the chordwise section at y are given by

$$\frac{L'(y)}{\rho(U_R)^2(c/2)} = (L_1+iL_2)\left(\frac{2z'_f}{c}\right) + (L_3+iL_4)\alpha'$$

$$= \left(\frac{\Omega R}{U_R^2}\right)\left(\frac{2R}{c}\right)\left(i\frac{p}{\Omega}\int_{x'_\ell}^{x'_t} k'dx' + U'k'_t\right) \qquad (23)$$

$$\frac{M'(y)}{\rho(U_R)^2(c/2)} = (M_1+iM_2)\left(\frac{2z'_f}{c}\right) + (M_3+iM_4)\alpha'$$

$$= \left(\frac{\Omega R}{U_R^2}\right)\left(\frac{2R}{c}\right)^2\left[U'\left(\int_{x'_\ell}^{x'_t} k'dx' - k'_t x'_t\right) - i\frac{p}{\Omega}\int_{x'_\ell}^{x'_t} k'x'dx'\right] \qquad (24)$$

where c is the local chord, U_R is a reference velocity, z'_f and α' are the local amplitudes of the flapping and twisting motions respectively, and L_1, L_3, M_1, M_3, and L_2, L_4, M_2, M_4, are the in phase and out of phase airload coefficients, respectively.

Expressions for Aerodynamic Influence Coefficients

Forward Flight (Rotor Blade at $\psi = \pi/2$)

The influence coefficients are calculated by the method outlined in Ref. 18. For a box not containing the collocation point

$$S_{ij} = -\int_{y'_j-d_2}^{y'_j+d_2}\int_{x'_i-d_1}^{x'_i+d_1}\left(\frac{e^{-i\kappa' r'_s}}{r'^3_s}\right)\beta(1+i\kappa' r'_s)dx'dy' \qquad (25)$$

where $\kappa' = \frac{M\rho}{\beta^2\Omega U'_j}$, $r'_s = [(x'-x'_m)^2 + \beta^2(y'-y'_n)^2]^{1/2}$, $d_1 = \Delta x'/2$, $d_2 = \Delta y'/2$, and $\Delta x'$ and $\Delta y'$ are the chordwise and spanwise spacings of the rectangular grid on the surface of the rotor blade. When the collocation is inside the box considered, the value of S_{ij} must be calculated by the method of Ref. 18. For the curved wake

$$T_j = -\int_{n'_j-d_2}^{n'_j+d_2}\int_{s'_t}^{\infty} e^{-i\frac{\nu'(s'-s'_t)}{q'}}\left(\frac{e^{-i\kappa' r'_w}}{r'^3_w}\right)\beta[(1+i\kappa' r'_w)\left(1-\frac{3\beta^2 z'^2}{r'^2_w}\right) + \kappa'^2\beta^2 z'^2]\,ds'dn' \qquad (26)$$

where $r'_w = [(x'-x'_m)^2 + \beta^2(y'-y'_n)^2 + \beta^2 z'^2]^{1/2}$, $x' = \mu\theta + y'_j \sin\theta$, $y' = y'_j\cos\theta$, $z' = d'\theta/2\pi$, $ds' = (dx'^2+dy'^2)^{1/2} = (\mu^2+y'^2_j+2\mu y'_j\cos\theta)^{1/2}d\theta$, and $d(=Rd')$, the downward displacement of the wake per revolution, is assumed to be small. T_j's are evaluated numerically at the j'th spanwise strip by taking small increments of θ and n.

Hovering Flight (Low Inflows)

For hovering flight, $\mu = 0$, $s' = y'_j\theta$, and $ds' = y'_j d\theta$. The expression for S_{ij}, Eq. (25), can be simply modified by replacing μ with zero and the wake integration for the j'th strip

$$T_j = -\int_{n'_j-d_2}^{n'_j+d_2}\int_{\theta_t}^{\infty} e^{-i\nu'(\theta-\theta_t)}\left(\frac{e^{-i\kappa' r'_w}}{r'^3_w}\right)\beta[(1+i\kappa' r'_w)\left(1-\frac{3\beta^2 z'^2}{r'^2_w}\right) + \kappa'^2\beta^2 z'^2]\,y'_j\,d\theta dn' \qquad (27)$$

where $x' = y'_j \sin\theta$, $y' = y'_j\cos\theta$, and $z' = d'\theta/2\pi$.

The effect of the helical wake in hovering flight is estimated by two different methods. In the first method, a Helical Wake Model is used and the actual helical path is taken in evaluating the T_j coefficients. In the second method, a Circular Wake Model is employed and the helical wake is replaced by its near wake, which is assumed to extend over $\theta_t \le \theta \le \pi/2$, and a number of regularly spaced circular disks of vorticity below the reference plane. The formula for k' for the n'th disk at $z' = nd'$ is taken to be simply

$$k'(\theta, y', nd') = k'_t(y')e^{-i\frac{p}{\Omega}[(\theta-\theta_t)+2n\pi]}, \qquad (28)$$

the actual spacing between consecutive disks being Rd'.

Results and Discussion

A rectangular rotor blade of R/c = 10 was chosen and the blade was assumed to extend from 0.1R to R. For the computation of the airload coefficients, a grid of thirty six rectangular boxes consisting of six chordwise and six spanwise stations were used. The convergence of the results was tested by taking grid sizes of 6x8 (chordwise x spanwise) and 8x6. Rigid mode shapes for flapping and twisting oscillations are assumed so that

$$\zeta = \gamma y' + \alpha x'$$

$$w'(x'_p, y'_p) = \Omega R[\alpha'(\mu+y'_p+i\frac{p}{\Omega}x'_p) + \gamma' i\frac{p}{\Omega}(\mu+y'_p)]$$

$$= \Omega R[(\mu+y'_p+i\frac{p}{\Omega}x'_p)\alpha' + i\frac{p}{\Omega}(\mu+y'_p)\left(\frac{c}{2R}\right)\left(\frac{2z'_f}{c}\right)]. \qquad (29)$$

It should be noted that the above equation is valid only for the blade position at $\psi = \pi/2$. For hovering flight, $\mu = 0$ in Eq. (29).

The airload coefficients for Mach numbers 0 0.8 for several values of $\frac{p}{\Omega}$ and wake spacing of two chords were obtained with reference to the blade's quater-chord axis. In Figs. (2) thru (5), selected airload coefficients for slow forward flight (μ = 0.1) are compared with the results obtained for hovering flight using both a helical wake model and two-dimensional strip theory. For this particular comparison, the reference velocity in Eqs. (23) and (24) was taken as the relative local velocity, U, and the tip Mach number was 0.8. From these plots, one can conclude that strip theory predicts substantially larger values for the airload coefficients. One of the most important observations one can make is that the curved wake changes the chordwise load distribution in such a way that the center of pressure shifts forward of the quarter-chord axis position (see Fig. 4).

Figs. (6) and (7) compare the results by several mathematical models used for the hovering flight case. The airload coefficients are referred to the tip velocity (ΩR) and this choice was made to indicate the trends of spanwise load distribution. The Circular Wake model representation results in a substantial saving in computational time. For example, to obtain the airload coefficients for one set of geometric and flight conditions using 6x6 grid on the blade, the Circular Wake model took only 1.5 minutes of computing time on IBM 360/65 while the Helical Wake model took 2.5 minutes. Although the Circular Wake model seems to indicate the general trends of the airload coefficients, one should use the full helical wake to compute the airload coefficients accurately.

Some typical results for hovering flight using the Circular Wake representation, compared with the results of two-dimensional strip theory, Ref. 7, are shown in Figs. (8) thru (11). The results for the curved wake are in good agreement with the results for strip theory for the inner blade sections; however, the agreement is poor towards the tip. Figs. (12) and (13) show the variation with axis position of M_4, conveniently referred to as pitching moment damping airload coefficient, at spanwise stations of 0.475R and 0.925R, respectively. From these results, one can conclude that the agreement between the curved wake results and strip theory is good near the quarter-chord position for M = 0 and M = 0.8 but it becomes very poor as the axis is moved towards the trailing edge.

References

1. Jones, W. P., McCrosky, W. J., and Costes, J. J., "Unsteady Aerodynamics of Helicopter Rotor Blades," NATO AGARD Report No. 595, April 1972.
2. Jones, J. P., "The Influence of the Wake on the Flutter and Vibration of Rotor Blades," Aeronautical Quarterly, Vol. IX, August 1958.
3. Daughaday, H. and Kline, J., "An Investigation of the Effect of Virtual Delta-Three Angle and Blade Flexibility on Rotor Blade Flutter," Cornell Aeronautical Laboratory Report, SB-86 2-5-2, August 1954.
4. Loewy, R. G., "A Two-Dimensional Approximation to the Unsteady Aerodynamics of Rotary Wings," Journal of the Aeronautical Sciences, Vol. 24, No. 2, February 1957, pp. 81-92.
5. Timman, R. and Van de Vooren, A. I., "Flutter of a Helicopter Rotor Ratating in its Own Wake," Journal of the Aeronautical Sciences, Vol. 24, No. 9, September 1957, pp. 694-702.
6. Jones, W. P., "Aerodynamic Forces on Wings in Non-Uniform Motion," R&M No. 2117, 1945, British Aeronautical Research Council.
7. Jones, W. P. and Rao, B. M., "Compressibility Effects on Oscillating Rotor Blades in Hovering Flight," AIAA Journal, Vol. 8, No. 2, February 1970, pp. 321-329.
8. Jones, W. P., "The Oscillating Airfoil in Subsonic Flow," R&M No. 2921, 1956, British Aeronautical Research Council.
9. Hammond, C. E., "Compressibility Effects in Helicopter Rotor Blade Flutter," GITAER Report 69-4, December 1969, Georgia Institute of Technology, School of Aerospace Engineering.
10. Ashley, H., Moser, H. H., and Dugundji, J., "Investigation of Rotor Response to Vibratory Aerodynamic Inputs, Part III, Three-Dimensional Effects on Unsteady Flow Through a Helicopter Rotor," WADC TR 58-87, October 1958, AD203392, U. S. Air Force Air Research and Development Command.
11. Reissner, E., "Effects of Finite Span on the Airload Distributions for Oscillating Wings, Part I - Aerodynamic Theory of Oscillating Wings of Finite Span," NACA Technical Note No. 1194, 1947.
12. Jones, W. P. and Rao, B. M., "Tip Vortex Effects on Oscillating Rotor Blades in Hovering Flight," AIAA Journal, Vol. 9, No. 1, January 1971, pp. 106-113.
13. Miller, R. H., "On the Computation of Airloads Acting on Rotor Blades in Forward Flight," Journal of the American Helicopter Society, Vol. 7, No. 2, April 1962, pp. 55-66.
14. Miller, R. H., "Unsteady Airloads on Helicopter Rotor Blades," Journal of the Royal Aeronautical Society, Vol. 86, No. 640, April 1964, pp. 217-229.
15. Miller, R. H., "Rotor Blade Harmonic Air Loading," AIAA Journal, Vol. 2, No. 7, July 1964, pp. 1254-1269.
16. Piziali, R. A., "A Method for Predicting the Aerodynamic Loads and Dynamic Response of Rotor Blades," USAAV-LABS Technical Report 65-74, January 1966, AD 628583.
17. Sadler, S. G., "A Method for Predicting Helicopter Wake Geometry, Wake Induced Flow and Wake Effects on Blade Airloads," presented at the 27th Annual National V/STOL Forum of the American Helicopter Society, Washington, D. C., May 1972.
18. Jones, W. P. and Moore, J. A., "Simplified Aerodynamic Theory of Oscillating Thin Surfaces in Subsonic Flow," AIAA Journal, Vol. 11, No. 9, September 1973, pp. 1305-1309.
19. Jones, W. P., "Oscillating Wings in Compressible Subsonic Flow," R&M No. 2885, October 19 55, British Aeronautical Research Council.
20. Shipman, K. W. and Wood, E. R., "A Two-Dimensional Theory for Rotor Blade in Forward Flight," Journal of Aircraft, Vol. 8, No. 12, December 1971, pp. 1008-1015.

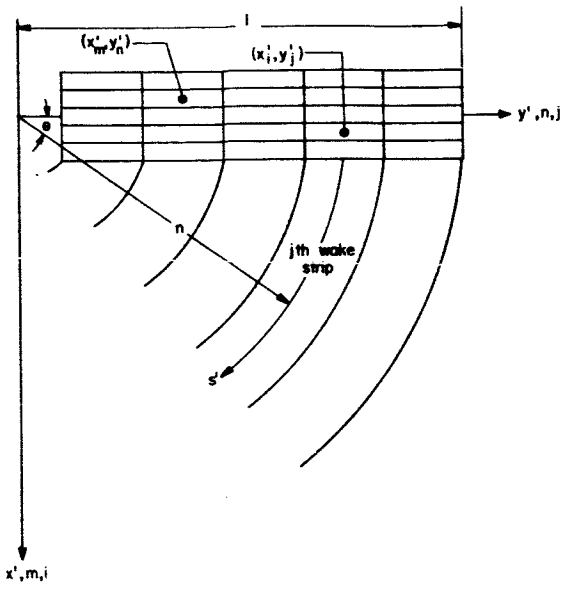

Fig. 1 Schematic Diagram of Rotor Blade and its Wake.

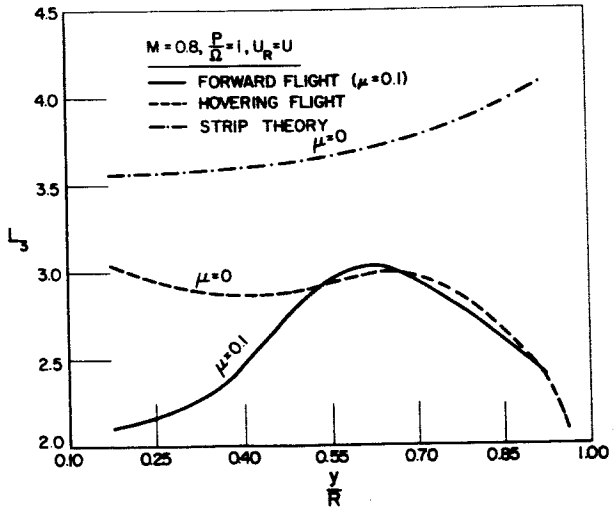

Fig. 2 Spanwise Variation of L_3.

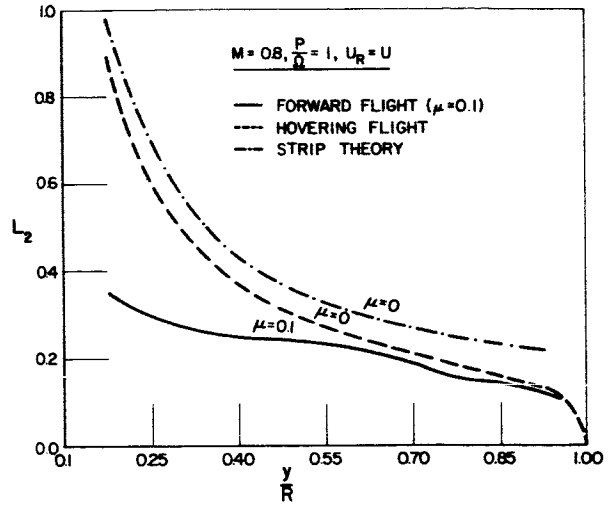

Fig. 3 Spanwise Variation of L_2.

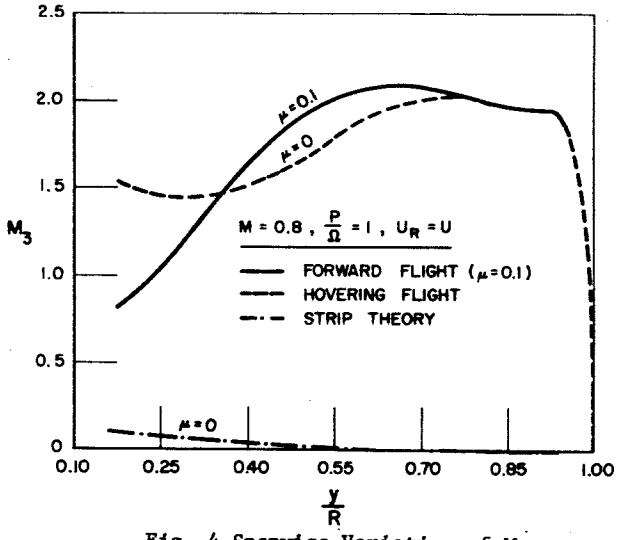

Fig. 4 Spanwise Variation of M_3.

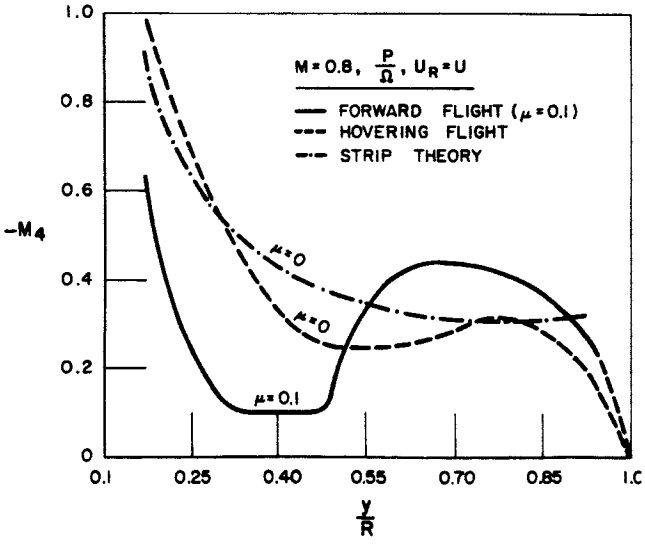

Fig. 5 Spanwise Variation of M_4.

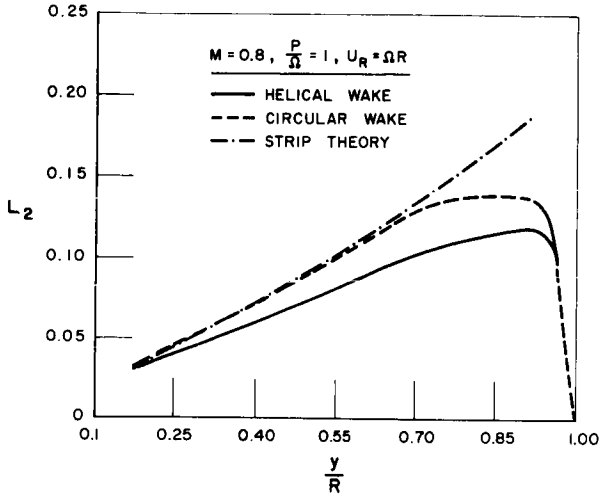

Fig. 6 Spanwise Variation of L_2 for Hovering Flight.

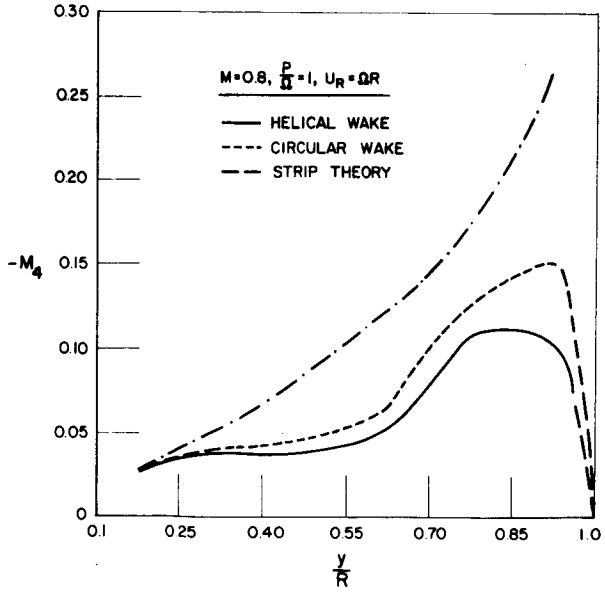

Fig. 7 Spanwise Variation of M_4 for Hovering Flight.

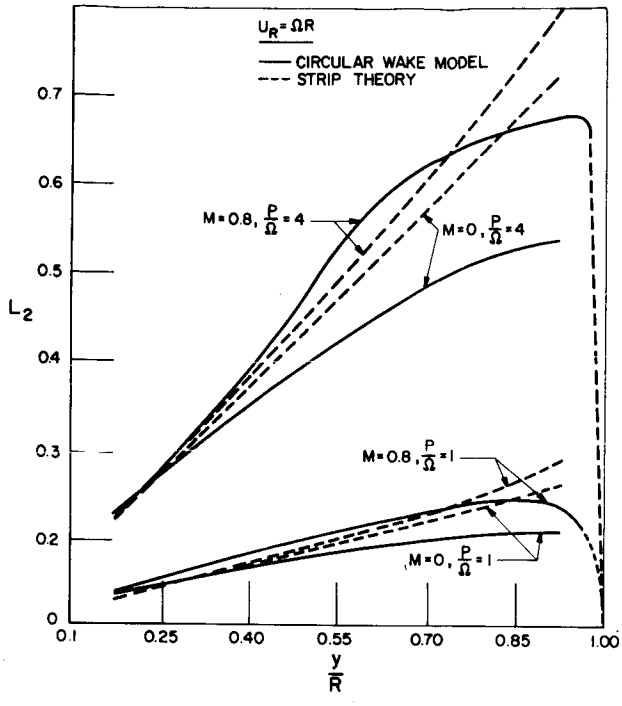

Fig. 8 Spanwise Variation of L_2 for Hovering Flight.

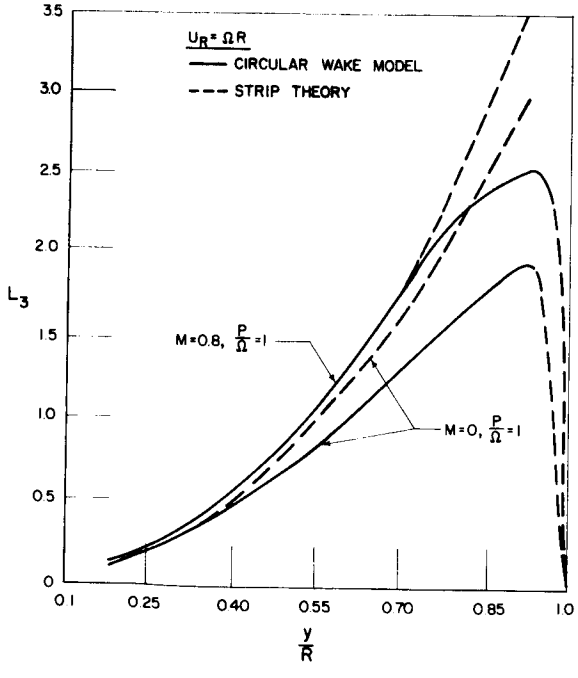

Fig. 9 Spanwise Variation of L_3 for Hovering Flight.

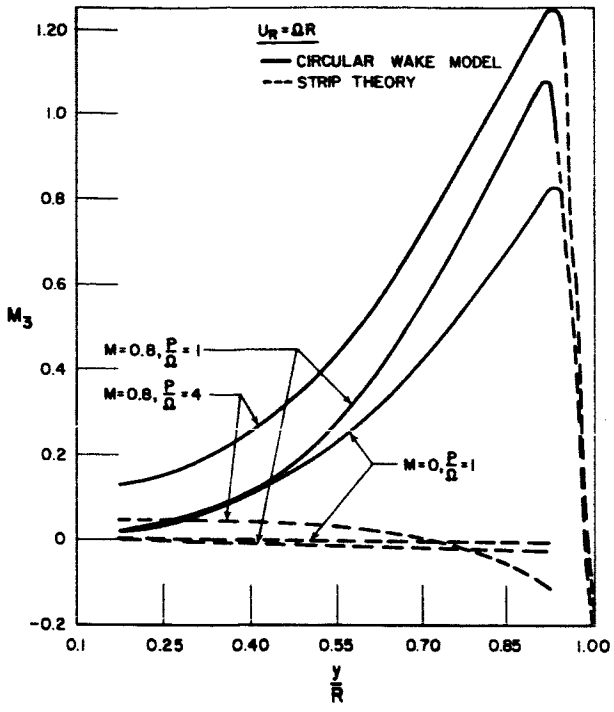

Fig. 10 Spanwise Variation of M_3 for Hovering Flight.

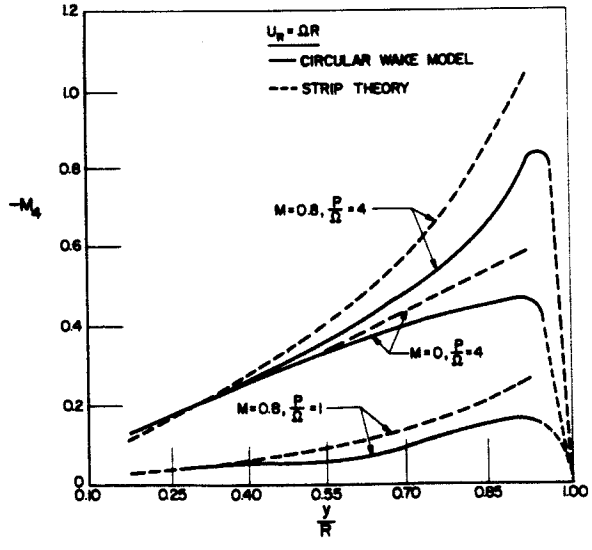

Fig. 11 Spanwise Variation of M_4 for Hovering Flight.

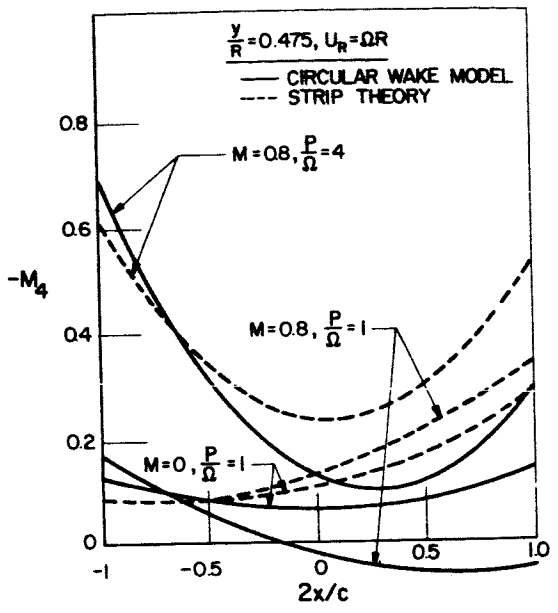

Fig. 12 Variation of M_4 With Reference Axis Position for Hovering Flight.

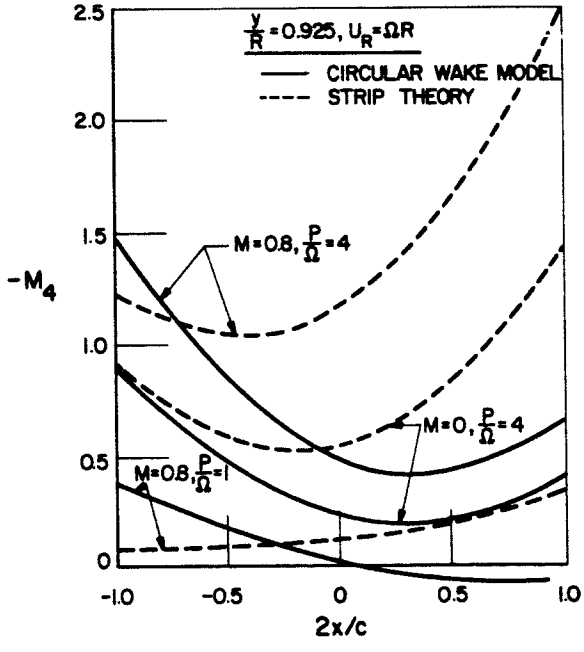

Fig. 13 Variation of M_4 With Reference Axis Position for Hovering Flight.